Electronic Supplementary Material (ESI) for Journal of Materials Chemistry

Supporting Information for —

A Rational Design for Donors in Organic solar cells: The Conjugated Planar Molecules Possessing Anisotropic Multibranches and Intramolecular Charge Transfer

Xue Yong and Jingping Zhang*

Faculty of Chemistry, Northeast Normal University, Changchun, 130024, China

Table of Contents

SI. Choice of methods

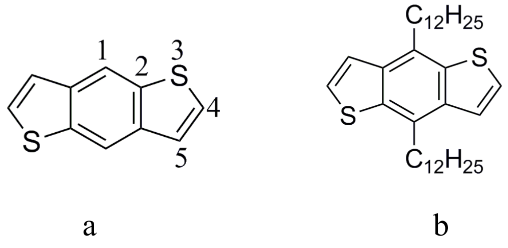

Scheme S1: Molecular structure of (a). Benzo[1,2-b′:4,5-b]-dithiophene (BDT) (b). 4,8-didodecylbenzo[1,2-b′:4,5-b]-dithiophene.

Table S1: Selected optimized geometrical parameters of BDT by using the PBE0/6-31G(d), B3P86/6-31G(d), and B3LYP/6-31G(d) Methods

	PBE0	B3P86	B3LYP	Exp[a]
B(1,2)/ Å	1.387	1.378	1.390	1.394
B(2,3)/Å	1.747	1.750	1.762	1.716
B(3,4)/ Å	1.738	1.741	1.754	1.730
A(1,2,3)/ °	126.8	126.8	126.8	127.8
A(2,3,4)/ °	91.1	91.1	90.9	90.5

[a] see Ref. S1

Although a good agreement for C-C bonds length (1.394 Å versus an experimental value of 1.394Å) and angles (126.8°, 90.9° vs. 127.8°, 90.5° of experimental[1] values respectively) can be obtained, the predicted C-S bonds length using B3LYP/6-31G(d) are found to deviate from their experimental values by about 0.46 and 0.24 Å. The PBE0 and B3P86 provide consistent results, while the results from the PBE0 agree better with the experimental dates (the observed deviation is less than 0.031 Å in bond length and less than 1 ° in bond angles).

Table S2: Calculated excitation energies (E_v), wavelength (λ_{ab}), and oscillator strength (*f*) of 4,8-didodecylbenzo[1,2-b′:4,5-b]-dithiophene calculated by Various Methods.

Method	E_v[a] (eV)	λ_{ab} (nm)	*f*
TD-PBE0/6-31G(d)	3.56	349	0.129
TD-B3LYP/6-31G(d)	3.43	361	0.114
TD-B3P86/6-31G(d)	3.92	316	0.176
exp[b]		347	

[a] the first lowest excitation energies, [b] see Ref. S2

From Table S2, while the calculated the maximum absorption wavelength was overestimated by about 14 nm using the TD-B3LYP/6-31G(d) but underestimated by about 31 nm with the TD-B3P86/6-31G(d), respectively, the TD-PBE0/6-31G(d) yields the most accurate result (349 vs. 347 nm of experiment value).[2]

SII. The choice of electron-deficient fragments (A_Fs)

Table S3 Calculated energy data of the frontier molecular orbitals of BDT, **B_F1_2-D_F-B_F2_2**, and the 6 A_Fs (A_F1-A_F6) (E_{HOMO}= HOMO energy levels; E_{LUMO}= LUMO energy levels; and E_g = E_{LUMO} - E_{HOMO})

Molecules	E_{HOMO}	E_{LUMO}	E_g (eV)	Molecules	E_{HOMO}	E_{LUMO}	E_g (eV)
BDT	-5.92	-1.10	4.82	A_F3	-7.37	-2.68	4.69
B_F1_2-D_F-B_F2_2	-5.05	-2.40	2.65	A_F4	-7.71	-2.58	5.12
A_F1	-7.83	-3.39	4.44	A_F5	-6.91	-2.20	4.71
A_F2	-7.85	-3.37	4.48	A_F6	-7.92	-1.40	6.52

SIII. Optimized geometry for **B_F1_2-D_F-B_F2_2**

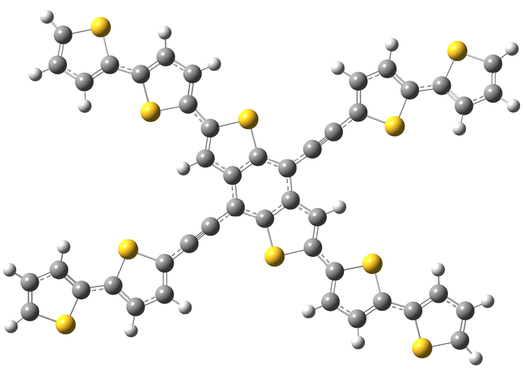

Fig. S1 The stereograph of optimized structures of the X-shaped **B_F1_2-D_F-B_F2_2**. (C, S, and H are shown in gray, yellow, and white, respectively)

SIV. Absorption properties for **X1, X2, B_F1_2-D_F-B_F2_2**, relative X-shaped derivatives based on A_F3-6, **PDI8**, and **PDI9**.

Table S4 Calculated excitation energies (E_v), wavelength (λ_{ab}), oscillator strength (*f*), and composition in terms of molecular orbitals with related character (H = HOMO, L = LUMO) for **X1**, **X2**, **PDI8**, and **PDI9**.

	Transition	E_v (eV)	λ_{ab} (nm)	*f*	Assignments
X1	S0→S1	1.67	732	0.966	H→L (0.96)(ICT)
	S0→S2	1.79	694	0.949	H→L+1(0.97)(ICT)
	S0→S5	2.05	605	1.693	H-1→L(0.87)(ICT)
	S0→S6	2.15	577	0.464	H-1→L+1(0.77)(ICT)
	S0→S10	2.31	536	0.529	H-2→L+2 (0.30)(ICT)
					H→L+4 (0.52)(π-π*)
	S0→S13	2.38	521	0.143	H-2→L+3 (0.91)(ICT)
	S0→S16	2.57	483	0.255	H-3→L+2 (0.89)(ICT)
	S0→S19	2.78	446	1.295	H→L+5(0.76)(π-π*)
	S0→S21	2.80	443	0.135	H-4→L(0.83)(π-π*)
	S0→S29	3.18	389	0.327	H-1→L+5(0.89)(π-π*)
X2	S0→S1	1.71	725	1.142	H→L(0.96)(ICT)
	S0→S2	1.84	675	1.203	H→L+1 (0.98)(ICT)
	S0→S5	2.07	598	2.052	H-1→L(0.90)(ICT)
	S0→S7	2.20	562	0.496	H-1→L+1(0.81)(ICT)
	S0→S10	2.39	519	0.426	H-2→L+2(0.41)(ICT)
					H→L+4(0.41)(π-π*)
	S0→S12	2.46	505	0.240	H-2→L+3(0.88)(ICT)
	S0→S16	2.65	470	0.430	H-3→L+2(0.86)(ICT)
	S0→S18	2.74	453	0.154	H-1→L+4(0.83)(π-π*)
	S0→S20	2.87	432	0.914	H→L+5(0.76)(π-π*)
	S0→S29	3.27	379	0.268	H-1→L+5(0.82)(π-π*)
PDI8	S0→S1	2.14	514(522)[a]	0.665	H→L (π-π*)
	S0→S15	4.46	278	0.330	H→L+4(0.77)(π-π*)
PDI9	S0→S1	2.44	509	0.689	H→L (π-π*)

[a]see Ref. S3

Table S5 Calculated excitation energies (E_v), wavelength (λ_{ab}), oscillator strength (*f*), and composition in terms of molecular orbitals with related character (H = HOMO, L = LUMO) for relative X-shaped derivatives based on A_F3-6, i.e., 1-(A_F3-B_F1)$_2$-D_F-(B_F2-A_F3)$_2$, 2-(A_F3-B_F1)$_2$-D_F-(B_F2-A_F3)$_2$, (A_F4-B_F1)$_2$-D_F-(B_F2-A_F4)$_2$, (A_F5-B_F1)$_2$-D_F-(B_F2-A_F5)$_2$, and (A_F6-B_F1)$_2$-D_F-(B_F2- A_F6)$_2$

	Transition	E_v (eV)	λ_{ab} (nm)	*f*	Assignments
1-(A_F3-B_F1)$_2$-D_F-(B_F2-A_F3)$_2$	S0→S1	1.85	669	1.283	H→L (0.95)
	S0→S2	2.01	617	1.223	H→L (0.95)
	S0→S16	2.88	430	0.685	H→L+5 (0.67)
2-(A_F3-B_F1)$_2$-D_F-(B_F2-A_F3)$_2$	S0→S1	1.88	657	1.012	H→L (0.93)
	S0→S3	2.01	615	0.936	H→L+2 (0.94)
	S0→S5	2.23	556	1.502	H-1→L (0.83)
	S0→S16	2.77	448	0.981	H-3→L+1(0.55)
(A_F4-B_F1)$_2$-D_F-(B_F2-A_F4)$_2$	S0→S1	1.96	633	1.283	H→L (0.95)
	S0→S2	2.19	566	1.456	H→L (0.95)
	S0→S16	2.31	536	1.933	H-1→L (0.91)
(A_F5-B_F1)$_2$-D_F-(B_F2-A_F5)$_2$	S0→S1	1.98	624	1.335	H→L (0.94)
	S0→S2	2.21	560	1.771	H→L+1 (0.88)
	S0→S16	2.87	432	1.220	H→L+5 (0.64)
(A_F6-B_F1)$_2$-D_F-(B_F2-A_F6)$_2$	S0→S1	2.12	586	1.415	H→L (0.97)
	S0→S15	3.37	368	0.608	H-2→L+3(0.72)

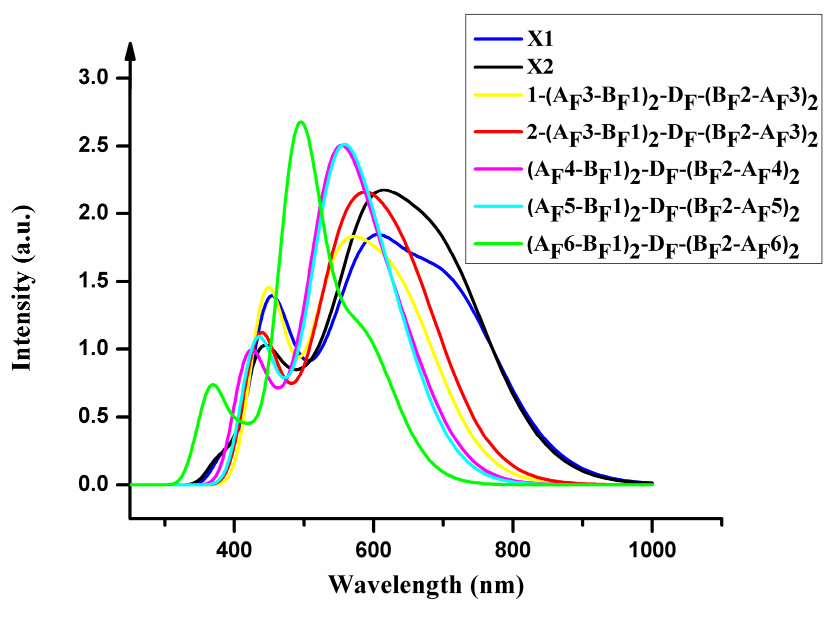

(a)

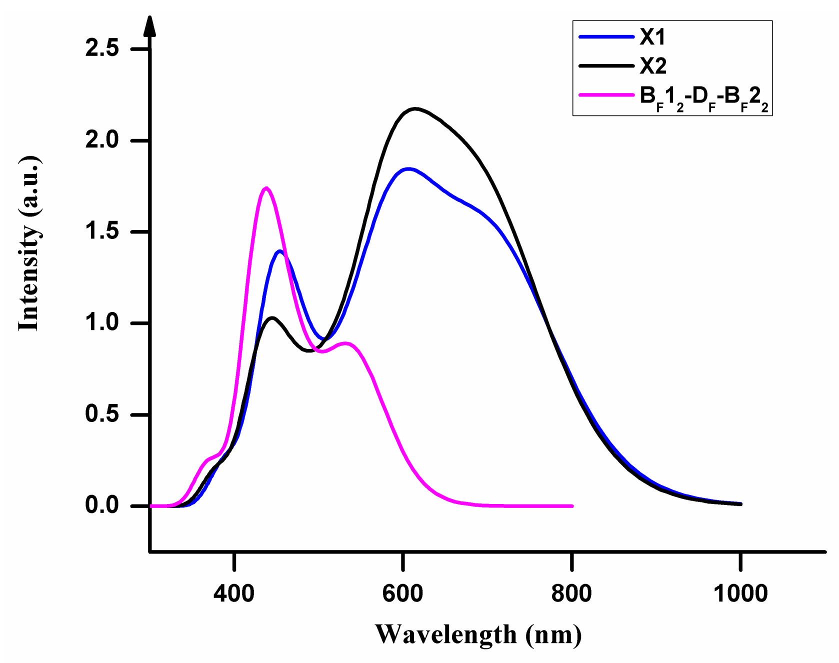

(b)

Fig. S2 (a) Simulated absorption spectra of 1-(A_F3-B_F1)$_2$-D_F-(B_F2-A_F3)$_2$, 2-(A_F3-B_F1)$_2$-D_F-(B_F2-A_F3)$_2$, (A_F4-B_F1)$_2$-D_F-(B_F2-A_F4)$_2$, (A_F5-B_F1)$_2$-D_F-(B_F2-A_F5)$_2$, and (A_F6-B_F1)$_2$-D_F-(B_F2-A_F6)$_2$; and (b) Simulated absorption spectra of **X1**, **X2**, and **B_F1$_2$-D_F-B_F2$_2$** at the TD-PBE0/6-31G(d) level.

Fig. S2a shows that the absorption spectra of **X1** and **X2** display two wider and stronger band in the whole visible and near-infrared region of the solar spectrum, whereas all the seven derivatives exhibit similar. The order of the excitation energy obtained at the TD-PBE0/6-31G(d) level is **X1** < **X2** < 1-(A_F3-B_F1)$_2$-D_F-(B_F2-A_F3)$_2$ < 2-(A_F3-B_F1)$_2$-D_F-(B_F2-A_F3)$_2$ < (A_F4-B_F1)$_2$-D_F-(B_F2-A_F4)$_2$ < (A_F5-B_F1)$_2$-D_F-(B_F2-A_F5)$_2$, <(A_F6-B_F1)$_2$-D_F-(B_F2-A_F6)$_2$ (1.67 < 1.71 < 1.85 < 1.88 < 1.96 < 1.98 < 2.12 eV). Hence, the excitation energy increases along with the decrease of the electron-withdrawing strength of the electron-accepting units. Therefore, both **X1** and **X2** exhibit superior absorption properties when compared with the other derivatives.

SV. Molecular orbitals for **X1**, **X2**, and **B_F1$_2$-D_F-B_F2$_2$**.

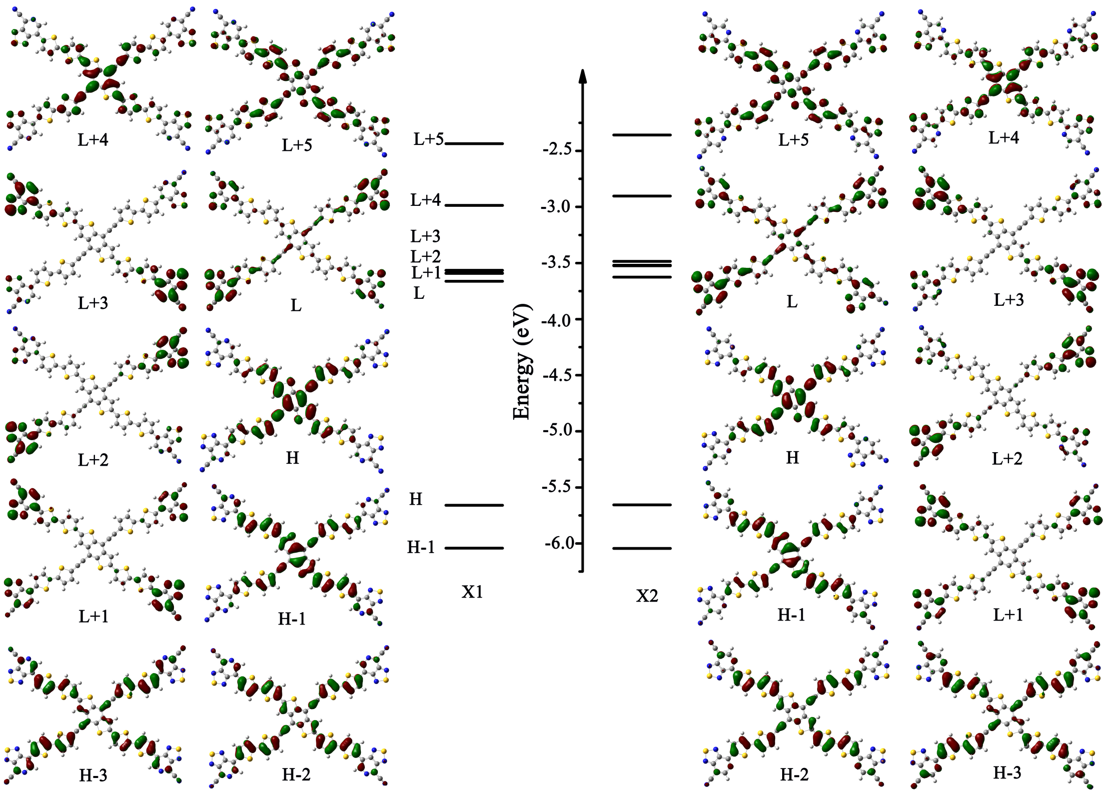

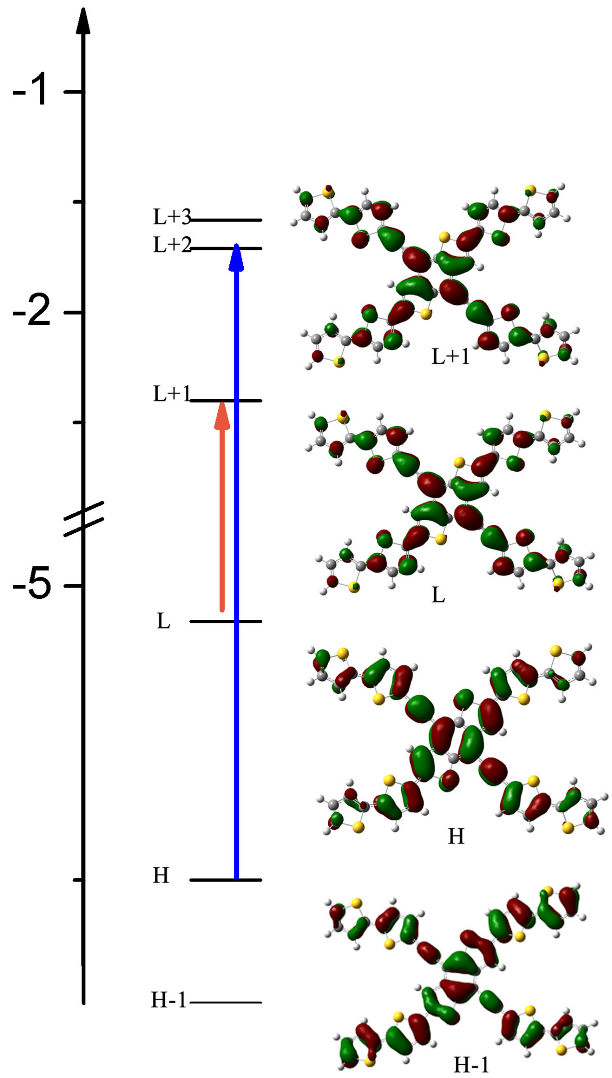

Fig. S3 Electron density plots of the FMOs of **X1**, **X2**, and $\mathbf{B_F1_2\text{-}D_F\text{-}B_F2_2}$ obtained by the PBE0/6-31G(d) method. (H = HOMO, L = LUMO). Arrow indicates main configuration of the strongest electronic excitations.

Table S6 Molecular orbital compositions (in percentage) of **X1** and **X2** (D_F = electron-rich fragment. B_F1 = π-bridge1, B_F2 = π-bridge2, and A_F = electron-deficient fragment)

		D_F	B_F2	B_F1	A_F
X1	L+5	16	32	32	20
	L+4	30	32	17	21
	L+3	1	2	12	84
	L+2	1	14	2	83
	L+1	1	16	11	83
	L	5	15	7	73
	H	36	38	19	7
	H-1	20	27	40	13
	H-2	17	8	36	17
	H-3	23	34	41	31
X2	L+5	17	30	30	23
	L+4	29	29	16	26
	L+3	2	5	16	77
	L+2	1	18	5	76
	L+1	2	9	14	75
	L	7	20	10	63
	H	36	38	19	7
	H-1	21	26	40	13
	H-2	38	9	36	17
	H-3	30	5	41	24

SVI. Match between the donor and acceptor

Table S7 Calculated energy data of the frontier molecular orbitals of **X1**, **X2**, and potential PDIs acceptors (E_{HOMO}= HOMO energy levels; E_{LUMO}= LUMO energy levels; and $E_g = E_{LUMO} - E_{HOMO}$)

Molecules	E_{HOMO}	E_{LUMO}	E_g (eV)	Molecules	E_{HOMO}	E_{LUMO}	E_g (eV)
X1	-5.66	-3.66	2.00	**PDI5**	-6.81	-4.05	2.76
X2	-5.65	-3.63	2.02	**PDI6**	-6.78	-4.02	2.76
PDI1	-6.75	-4.00	2.75	**PDI7**	-6.82	-4.03	2.79
PDI2	-6.81(-6.04)	-4.02(-4.07)[a]	2.79	**PDI8**	-6.69	-3.94	2.75
PDI3	-6.84	-4.08	2.76	**PDI9**	-6.76	-3.97	2.79
PDI4	-6.82	-4.06	2.76				

[a] see Ref. S4

SVII. Reorganization Energies and Stabilities

Table S8 Reorganization energies (λ_e/λ_h for electron/hole) for **X1**, **X2**, **PDI8**, and **PDI9**.

	X1	**X2**	**PDI8**	**PDI9**	TPD	Alq_3
λ_h (eV)	0.119	0.114	0.156	0.175	0.290[a]	
λ_e (eV)	0.062	0.056	0.257	0.263		0.276[b]

[a] see Ref. S5; [b] see Ref. S6

The calculated results provide λ_h values of 0.119 for **X1**, 0.114 for **X2**, 0.156 for **PDI8**, and 0.715 eV for **PDI9**; λ_e values of 0.062 for **X1**, 0.056 for **X2**, 0.257 for **PDI8**, and 0.263 eV for **PDI9**.

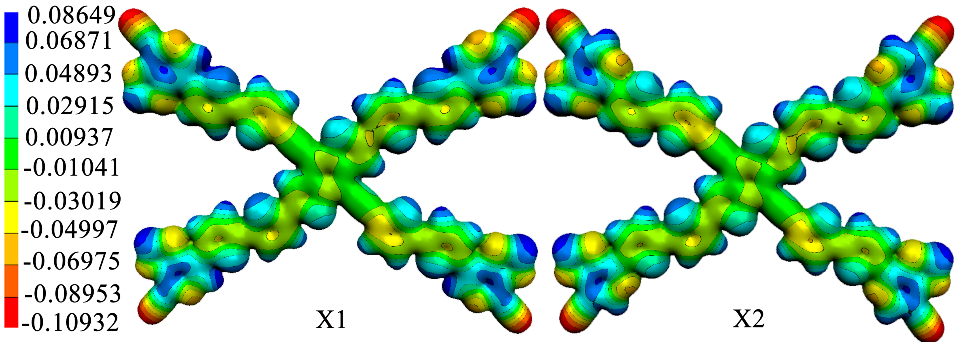

Fig. S4 Electrostatic surface potential (MEP) for **X1** and **X2**. Regions of higher electron density are shown in red and of lower electronic density in blue.

SVIII. Associated references

S1. K. Takimiya, Y. Konda, H. Ebata, N. Niihara and T. Otsubo, *J. Org. Chem.*, 2005, **70**, 10569.

S2. H. Pan, Y. Li, Y. Wu, P. Liu, B. S. Ong, S. Zhu and G. Xu, *Chem. Mater.*, 2006, **18**, 3237.

S3. B. A. Jones, A. Facchetti, M. R. Wasielewski and T. J. Marks, *Adv. Fun. Mater.*, 2008, **18**, 1329.

S4. W. S. Shin, H.-H. Jeong, M.-K. Kim, S.-H. Jin, M.-R. Kim, J.-K. Lee, J. W. Lee and Y.-S. Gal, *J. Mater. Chem.*, 2006, **16**, 384.

S5. M. Malagoli and J. L. Breas, *Chem. Phys. Lett.*, 2000, **327**, 13.

S6. B. C. Lin, C. P. Cheng, Z.-Q. You and C.-P. Hsu, *J. Am. Chem. Soc.*, 2004, **127**, 66.